THE JOURNAL OF PHYSICAL CHEMISTRY A

 VOLUME 112, NUMBER 45, NOVEMBER 13, 2008

CENTENNIAL FEATURE ARTICLE

Vibrational Relaxation of OH and CH Fundamentals of Polar and Nonpolar Molecules in the Condensed Phase†

Edwin L. Sibert III,* Sai G. Ramesh, and Tolga S. Gulmen

Department of Chemistry and Theoretical Chemistry Institute, University of Wisconsin—Madison, Madison, Wisconsin 53706

Received: July 31, 2008

Studies of vibrational energy flow in various polar and nonpolar molecules that follows the ultrafast excitation of the CH and OH stretch fundamentals, modeled using semiclassical methods, are reviewed. Relaxation rates are calculated using Landau−Teller theory and a time-dependent method, both of which consider a quantum mechanical solute molecule coupled to a classical bath of solvent molecules. A wide range of decay rates are observed, ranging from 1 ps for neat methanol to 50 ps for neat bromoform. In order to understand the flow rates, it is argued that an understanding of the subtle mixing between the solute eigenstates is needed and that solute anharmonicities are critical to facilitating condensed phase vibrational relaxation. The solvent-assisted shifts of the solute vibrational energy levels are seen to play a critical role of enhancing or decreasing lifetimes.

I. Introduction

A grand goal of physical chemistry is to measure and understand the flow of energy on the time scale of fundamental chemical processes, such as proton transfer, electron transfer, breaking and forming of hydrogen bonds, and stabilization of chemical intermediates following chemical reactions. Vibrational energy flow or relaxation (VER), both intra- and intermolecular, is an integral component of these processes, which motivates its experimental and theoretical investigation. Flow rates help us envisage the complex energy landscape of the systems under the microscope, and highlight the role of various couplings. This article is a review of our recent contributions to this expanding field.

Studies on dynamical events following the excitation of a high frequency oscillator in the condensed phase continue to attract the attention of experimentalists and theorists alike. These investigations have a 2-fold objective, viz. understanding the pathways by which the excitation energy is channelled into various intra- and intermolecular modes, and the role and control the solvent medium exerts on the observed rates. Using ultrafast lasers, experimentalists pump a nonstationary initial vibrational state, whose time evolution can be studied via probe pulses that allow the observation of population growth and decay in the modes of the excited molecule as well as neighboring solvent molecules.[1−34] These time profiles lead to the identification of primary acceptor modes and the most likely pathways for the decay of the excitation. Theoretical treatments complement the experiments, providing a molecular description of the relaxation process.[35−52]

† This year marks the Centennial of the American Chemical Society's Division of Physical Chemistry. To celebrate and to highlight the field of physical chemistry from both historical and future perspectives, *The Journal of Physical Chemistry* is publishing a special series of Centennial Feature Articles. These articles are invited contributions from current and former officers and members of the Physical Chemistry Division Executive Committee and from *J. Phys. Chem.* Senior Editors.

* To whom correspondence should be addressed. E-mail: sibert@chem.wisc.edu.

10.1021/jp8068442 CCC: $40.75
Published on Web 10/15/2008

Edwin L. Sibert, III is a Professor of Chemistry at the University of Wisconsin at Madison. Degrees include a B.A. (1978) from Colgate University in chemistry and a Ph.D. (1983) from the University of Colorado at Boulder in chemical physics. Sibert was a NATO Fellow at Oxford and a Miller Fellow at Berkeley before moving to Madison in 1986. Sibert is a theoretical chemist whose research interests include small molecule vibrational dynamics and the corresponding spectroscopy of the vibrational states, implementation of nondegenerate perturbation theory, statistical treatments of molecular vibrations, nonadiabatic dynamics of association reactions, and the quantum-classical correspondence principle. Recently the major focus of the group has been vibrational relaxation in liquids and double proton tunneling dynamics.

Sai G. Ramesh obtained his bachelor's degree in chemistry in 1999 from SIES college, Bombay. Joining Indian Institute of Technology, Bombay, he completed the master's degree program in chemistry in 2001, specializing in physical chemistry. He then moved to the University of Wisconsin—Madison for a doctoral program in theoretical chemistry. His thesis work, under the tutelage of Prof. Edwin Sibert, III, was mainly on the vibrations of bromoform in the gas and condensed phases. Since receiving his Ph.D. degree in 2006, he has been a post-doctoral researcher with Prof. James T. Hynes at the École Normale Supérieure, Paris. His general interests lie in classical and quantum treatments of small systems and model problems, including gas and solution phase dynamics.

Tolga S. Gulmen received a B.S. in 1999 from The College of William and Mary and a Ph.D. in 2005 from the University of Wisconsin under the tutelage of Edwin L. Sibert, III. He then moved on to a postdoctoral research position at the University of Kansas and worked on understanding properties of nanoconfined solvents in the laboratory of Ward H. Thompson. Currently, he is a student at the University of California, Berkeley, School of Law.

The rates and pathways of energy redistribution exhibit rich variations depending on the nature of both the solute and the solvent. The number of possible relaxation pathways increases significantly as the complexity of the solute vibrational structure increases. However, that need not imply faster rates: The strength of the solute−solvent interaction must also be considered. Hydrogen-bonding or highly polar liquids are at one extreme in this regard. OH excitation in liquids like H_2O[2,3,16,24,27,38,39,42,53,54] and CH_3OH[6,44−46,55−57] decays on a time scale of the order of 1 ps, with the latter species involving several pathways. The other extreme is comprised of weakly interacting species, such as halogenated methanes and hydrocarbons.[5,8,11−14,20,21,41,43] Their decay behavior is generally slower, with timescales running into tens of picoseconds.

For these reasons, it is important to study a range of systems so that various possible trends that may be present are revealed. Toward this end, we have theoretically investigated the vibrational relaxation of CH and OH stretches in several molecules and environments over the past few years. We have modeled CH relaxation in neat liquid chloroform,[43] bromoform,[50,51] and deuterated bromoform,[51] as examples of solute molecules weakly interacting with their environment. We have studied OH excitation decay in neat methanol[44] as an example of relaxation in a hydrogen bonding environment. To further clarify the environmental factors, we have investigated dilute methanol and deuterated methanol in carbon tetrachloride.[44,46] Direct non-equilibrium simulations have been carried out to clarify the quantum nature of the process.[52] Given the above solute molecules, a distinguishing feature of our work is that we may have over a thousand possible acceptor states into which the excitation may decay. We have focused on determining the solute−solvent coupling between these states, and developing simple frameworks for understanding the resulting timescales predicted by our models. In this article, we review these works in the context of ongoing research.

The outline of this paper is as follows. Section II provides an historical perspective on the field of vibrational relaxation. In section III, the experimental background is summarized. This section also contains an illustration of possible coupling scenarios, with chloroform chosen as the example. The semi-classical models we have used to describe vibrational relaxation pathways are explained in section IV. This is followed by a presentation and discussion, in section V, of key results from our calculations on methanol and the haloforms. Section VI offers some comments on future directions of VER research.

II. Historical Perspective

The experimental realization of vibrational relaxation measurements was spurred by the advent of picosecond spectroscopic methods around the early 70s. Among the first works was that of Alfano and Shapiro[58] on how the methyl vibrations of ethanol are de-excited, measured, for the first time, using stimulated Raman scattering. Several studies rapidly followed,[59−61] their number and system variety increasing with improvements in laser techniques and temporal resolution.[2,10,13,14,20−22,31,54,62−77] Morresi[1] and Deàk et al.[4] and, more recently, Pang et al.[29] and Elles and Crim[25] have reviewed these developments as well as the current challenges.

Key to many of the advances in this area was the development of the theoretical framework for describing vibrational energy relaxation (VER) in liquids; see, for example, ref 78 and references therein. Although one must be aware of its limitations,[78] Landau−Teller (LT) theory has emerged as the theory of choice. The works of Oxtoby[79,80] lay the groundwork work for implementation of the LT approach. Particularly noteworthy among the early studies was the pioneering work of Whitnell et al.,[35] who demonstrated the accuracy of LT theory for describing vibrational relaxation in liquids by comparing the results of this theory to nonequilibrium molecular dynamics (MD) simulations. The use of MD simulations to provide the input needed to calculate the friction, a key ingredient of LT theory, provided a quantitative advance its power to predict vibrational relaxation rates.

VER studies have ranged from diatomics[81−91] to proteins[28,33,37,47,48,65,70−72] as the target solutes. Those with a simple vibrational level structure are conceptually more tractable in that energy flow between only a few states, or merely two, need to be handled. However, the flip side is that a large amount of energy, typically well above kT, would have to be accommodated by the solvent bath as the solute transitions between its energy levels. A classic example is that of O_2 relaxation.[88,89] Quantum effects are significant in such cases, particularly if the solvent lacks modes with excitation frequencies close to this solute transition gap. These effects present fascinating challenges in their own right and represent an important and ongoing facet of research in the area of vibrational relaxation. Many paths have been adopted by workers in this branch, ranging from the use of well-chosen quantum correction factors,[42,87,92−96] to better, more computationally involved semiclassical approaches.[91,97−103]

An advantage of the simple intramolecular aspect of small molecules is that it allows one to focus on the solvent itself. In their pioneering work on HgI relaxation in ethanol, Gnanakaran and Hochstrasser[85] were able to elucidate how ethanol's structure and dynamics around HgI contribute to the relaxation time. More recently, Seifert and co-workers[16,30] studied relaxation of the bend fundamental of HOD in different solvents. The decay can only be to the ground vibrational state, and this enabled theory[57] to highlight solvent effects—particularly the possibility that it accepts energy leaving the solute into its intramolecular modes—less ambiguously than if there had been multiple decay paths.

This possibility of multiple intramolecular decay paths is what grows in very rapidly with polyatomic solutes. Experimental

works show that polyatomic molecules can vibrationally cool,[64] this making the VER process qualitatively different from that of diatomics. A stepwise decay is typically observed, in which intramolecular vibrational states at energies near that of the excited mode are populated shortly after excitation. As the solute finds its way to the ground-state through its vibrational manifold, the bath couples the decaying and accepting modes at each stage, and also takes up (pitches in) the excess (deficit) energy. This energy gain (loss) at each step is typically well under kT, so that quantum effects are not very significant.

The first realistic theoretical picture of such a process was obtained for the HOD molecule by Rey and Hynes.[38] Treating OH relaxation of HOD in a bath of D_2O, it was found that energy flows from the OH fundamental to the lower energy overtone of the bending degree of freedom, which in turns decay to other lower lying states. Rey and Hynes[38,39] were also the first to elucidate the role of vibrational anharmonicity of the solute molecule. They found that the accurate treatment of the intramolecular dynamics was essential for even a qualitative treatment of the decay rates. From a theoretical perspective this was, and continues to be, daunting, since it is unclear that the quality of force fields in both the gas and liquid phases, while having improved dramatically over the past decade, are good enough to yield quantitative agreement with experiment. Morita and Kato[104] and Skinner and co-workers[42,57,105−107] further examined the role of the anharmonicity and the solute−solvent couplings and systematically have shown the importance of the proper treatment of such couplings.

The aforementioned computations were carried out on triatomic solutes, which already show nontrivial results. The theoretical works on methanol and the haloforms that we will review in this article clearly significantly step up the complexity of the solute's vibrational structure. For example, the OH stretch of HOD can relax to at most four states: the bend overtone, the bend and OD stretch fundamentals, and the ground state. The CH stretch of chloroform, $CHCl_3$, has on the order of a thousand states to which it can relax. Treating all of these possibilities is, of course, impractical. Thankfully, previously developed propensity rules enable us to greatly reduce this number to a small set of candidate states. Our calculations provide a test of these propensity rules and clarify which of the possible candidates states are in fact relevant. A notable feature of these studies is that the solute vibrational energy levels fluctuate with time due to the solvent interactions. We find that these solvent-induced fluctuations must be considered when there is a high density of candidate acceptor states in the vicinity of the excited state.[45,46]

Before closing the section, we touch upon yet another ongoing branch of VER research on large solutes, namely the limit at which they appears to relax, at least initially, as though in vacuum. A few years ago, several incisive works appeared that emphasized the influential contribution of intramolecular energy flow to condensed phase relaxation. For solutes with reasonably high densities of states at the energy of the prepared state, typically on the order of 10 states per wavenumber, the initial relaxation steps were found to be essentially intramolecular and uninfluenced by the solvent. Such behavior was observed clearly upon CH fundamental excitation in terminal acetylenes,[17−19] overtone excitation in iodomethanes,[20,21] and also in large macromolecular systems.[47,48] These systems remain a challenge to treat: The state density is prohibitive to quantum mechanical treatment at present. The studies addressed in this review encompass molecules with notably lower densities of states, with little vibrational relaxation observed in quantum calculations of the gas phase solute molecules.

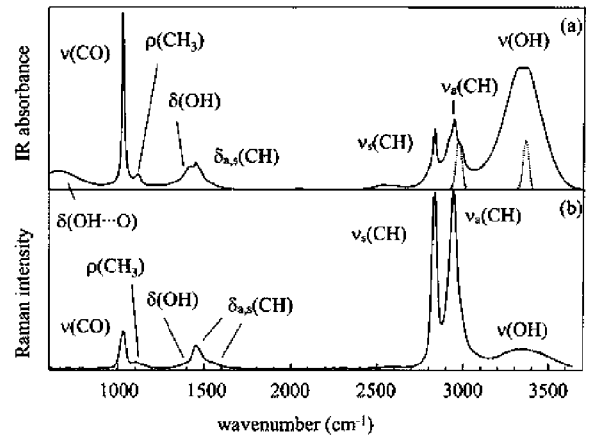

Figure 1. IR and Raman spectra of methanol, obtained by Iwaki and Dlott[6] with instrumental resolution better than the natural line widths. The assignments are from ref 137. The dotted curves under the CH and OH transitions are the spectral profiles of the mid-IR pump pulses.

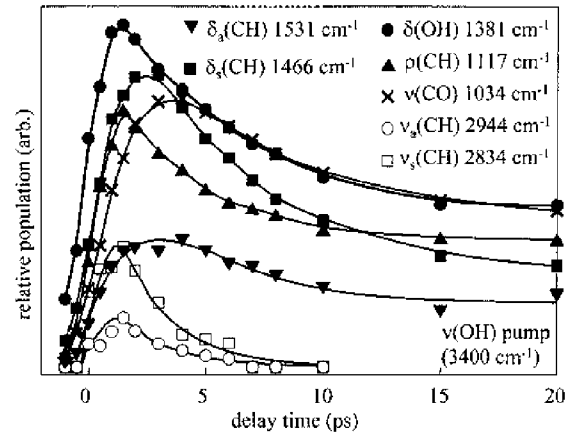

Figure 2. Population in the spectrally distinct normal modes as a function of time following 3400 cm^{-1} excitation of the OH stretch fundamental. Results are those of Iwaki and Dlott.[6] See their text for further details.

III. Background

We begin this section with a presentation of those experimental findings that are relevant to the theoretical results reviewed in this article. We then describe those features of the solute vibrational states that are central to understanding the relative importance of relaxation pathways.

In Figure 1 we show a spectrum of methanol with the major peaks assigned.[6] All vibrations are Raman active and can be spectrally resolved. To measure dynamics, Iwaki and Dlott[6] excite the OH stretch with an IR pump pulse whose frequency profile is shown in the top panel. The population is then probed using time-resolved anti-Stokes scattering. The observed signal is a measure of the population in the various fundamental levels. If the fundamental transition cannot be spectrally resolved from the transition between the fundamental to overtone, then more analysis is needed. Results for an excitation pulse centered at 3400 cm^{-1} are shown in Figure 2. Following this OH excitation pulse, there is flow on a ps time scale into essentially all of the vibrational modes of the molecule. Apparently, there are many acceptor states for probability flow.

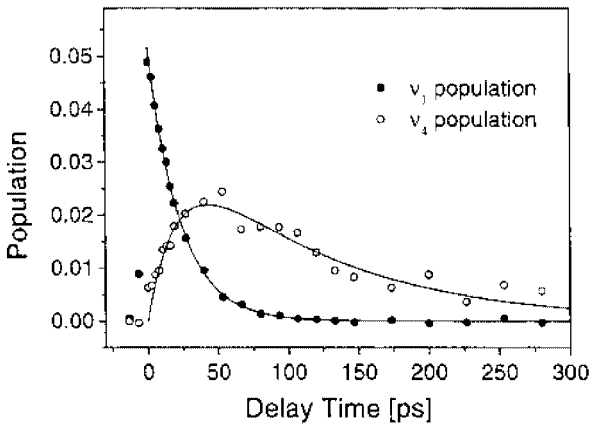

Figure 3. Time evolution of the CH stretching mode 1 (darkened circles) and of the CH bending mode 4 (open circles) population, following CH stretch excitation in $CHCl_3$. The points are experimental and the curve is fitted. Figure is from Graener et al.[10]

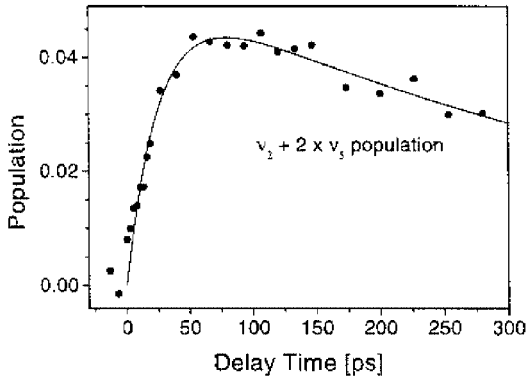

Figure 4. Time evolution, in chloroform, of population densities of the sum of the CCl_3 stretching populations $\nu_2 + 2\nu_5$ as a function of delay time: the points are experimental and the curve is fitted. Figure is from Graener et al.[10]

To contrast to the energy flow in methanol, we show results for energy flow in chloroform in Figures 3 and 4. The former figure shows probability flow out of the CH stretch on a 23 ps time scale. On the same time scale, probability flows into the bending degrees of freedom as well as the CCl stretching degrees of freedom. The latter flow is shown in Figure 4 as the total probability of being in a CCl stretch fundamental. There are two distinct stretching fundamentals, and probability apparently flows into the symmetric CCl stretch and then equilibrates between all three CCl stretching fundamentals on a time scale that is fast compared to the flow out of the CH stretch. The low frequency bends appear to be unexcited at short times.

The goal of theory is to elucidate these results, shedding light on the important factors that cause the observed flow patterns and rates. As mentioned above, Rey and Hynes[38,39] were the first to seriously examine the effect of the anharmonicity of the molecular vibrations. They demonstrated that the inclusion of realistic anharmonic potentials is crucial for a quantitative treatment of the decay rates. This finding can easily be understood in the context of LT theory. Here the time-dependent solute−solvent interactions serve to transfer probability between the solute vibrational energy levels, in much the same way as an electric field excites or de-excites molecules by transferring probability between energy levels. Using LT theory, Rey and Hynes calculated that the fastest decay path, following excitation of the OH stretch of HOD in D_2O, was to the bend overtone. If the normal mode picture were valid, i.e., no anharmonicities, one would need a solute−solvent coupling term linear in the OH normal mode and bilinear in the bend in order to couple these states. This high order coupling term is, as is expected, negligible. On the other hand, if anharmonicities were present, the initial OH stretch and final bend overtone would have small contributions from many normal mode states, and these states would allow the initial and final states to couple via solute−solvent terms that are linear in the solute normal mode. This is indeed the case.

TABLE 1: Energies of the Fundamentals of $CHCl_3$, $CHBr_3$, and $CDBr_3$ obtained in refs 43 and 111

		energy (cm^{-1})		
state	description	$CHCl_3$	$CHBr_3$	$CDBr_3$
$\nu_1(A_1)$	CH(D) str.	3033.4	3047.5	2272.6
$\nu_2(A_1)$	CX symmetric stretch	678.3	542.6	524.1
$\nu_3(A_1)$	"umbrella"	368.7	223.2	225.0
$\nu_4(E)$	CH(D) bend	1220.6	1148.2	853.2
$\nu_5(E)$	CX asymmetric stretch	776.2	669.7	646.9
$\nu_6(E)$	CX bend	260.0	155.0	155.0

The role of anharmonicity is significantly more pronounced for larger solute molecules. The time-dependent solute−solvent interactions are dominated by low-frequency components arising from the hindered translations and rotations of the molecules making up the liquid. One would thereby assume that the most likely transitions are to nearby energy levels. These levels, however, typically look very different than the initially excited mode. This difference can be quantified by the overall change in vibrational quanta between the initial and final states. It is defined as

$$\Delta v = |\mathbf{v} - \mathbf{v}'| \tag{1}$$

Here we are assuming that one can assign quantum numbers to both the initial and final states in terms of a separable basis set. These states are defined by the vectors $\mathbf{v}$ and $\mathbf{v}'$, respectively. In the limit of a harmonic oscillator linearly coupled to a bath, there is a rigorous $\Delta v = 1$ selection rule. Changes with $\Delta v \geq 2$, arise as a result of either higher order couplings between the solvent and solute or intramolecular anharmonicities. In the HOD relaxation, just described, $\Delta v = 3$. A guiding rule of thumb is that all other factors being equal, the larger the value of Δv, the slower the rate of vibrational relaxation. Offsetting this factor is the second quantity, the energy mismatch ΔE between the donor and acceptor states. The rate of energy transfer typically decreases exponentially as ΔE increases for solvents with no vibrational degrees of freedom due to the fact that the time-dependent solute−solvent motions are dominated by the low frequency motions mentioned above.

To apply the above ideas one needs, as a starting point, a basic picture of the energy levels of the solute molecule. At the very least, to determine these levels, one should know the normal-mode frequencies. One can combine these frequencies to find approximate energies of overtones and combinations bands. This directly gives the Δv and rough ΔE values for several donar–acceptor state pairs. These quantities are in turn used to make several predictions as to the expected pathways of energy flow. We now turn to the chloroform molecule to illustrate these ideas.

The frequencies for the chloroform molecule are given in Table 1. Figure 5 illustrates the decay routes that we believe to be the most likely. The following discussion of these routes are guided by the results of the experimental studies of Graener et al.[10] and Bakker et al.[8,108]

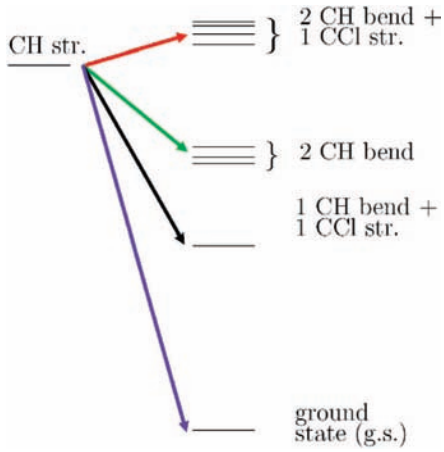

Figure 5. Schematic diagram showing four likely pathways for energy flow in chloroform. The two distinguishing features of these routes are the change in vibrational quanta Δv in going from the fundamental to the final states and the energy mismatch ΔE between the initial and final states. The states shown on the right represent a small subset of the more than 2000 possible vibrational states that could be involved in the decay process.

The first possibility corresponds to a loss of the quantum of CH excitation in a single step. This process has the largest ΔE and smallest Δv. For diatomics this is the only possible process. However, it has been found to be important in triatomics as well when the solvent−solute coupling is large. Morita and Kato[104] calculated that, for the relaxation of the asymmetric stretch of the azide ion in water, this pathway accounts for half of the total decay despite the large ΔE. In chloroform, however, this pathway is likely to be unimportant based on the experimental results. For this pathway, the rates of probability that flow out of the CH stretch fundamental and into the ground-state are the same, a result that is inconsistent with the experimental observations that the former rate is at least a factor of 6 faster.[8,10,108]

Figure 5 shows two $\Delta v = 3$ pathways. One of these corresponds to energy transferring from the CH fundamental to the CH bend overtone. This pathway has been observed in methanol,[6] although there the ΔE is smaller. For chloroform the energy mismatch is similar to that which is observed in the HOD study of Rey and Hynes,[38] where the dominant pathway involves population transfer from the OH stretch to bend overtone and $\Delta E = 500-600$ cm^{-1}. Moreover, this energy corresponds to that which would be needed to excite a water librational mode, and hence, these specific modes were predicted to play the role of acceptor modes. In $CHCl_3$ there are no intermolecular modes with such high frequencies. In fact, all of these modes involve low frequency hindered rotations and translations of the massive chloroform molecule. Therefore, this decay route, in which all of the excess energy is taken up by the solvent, is not likely. A CCl stretch has a frequency of about 700 cm^{-1}, so that the scenario of probability flowing out of the CH stretch and into the CH bend overtone, with the concomitant excitation of a CCl stretch on another chloroform molecule, appears to be more likely.

The second $\Delta v = 3$ pathway has an acceptor mode corresponding to excitation of one quantum of CH bend and one quantum of CCl stretch. This process has $\Delta E \sim 1100$ cm^{-1}, and based on the simple guidelines presented at the beginning of this section, this decay route is considerably less likely than the other $\Delta v = 3$ route described above, if all of the excess energy is to be taken up by the intermolecular solvent modes. However, if this decay path were accompanied by a concomitant excitation of a CH bend on a neighboring molecule, it then becomes more likely. Interestingly, the results of Graener et al.[10] support the scenario in which all of the excess energy goes into the intermolecular solvent modes. They observe that the CH bend and CCl stretches are populated on about the same time scale as that which the CH stretch loses energy. This frequency information does not serve to distinguish between the above two pathways, since both lead to excitation of CH bends and CCl stretches. Nevertheless, the experimental intensities do distinguish between them, since intensities correlate to absolute populations. The former decay route would lead to equal population in the CH bend and CCl stretch modes, whereas the latter would have double the population in the CH bend. Graener et al.[10] observe equal populations.

The final pathway shown in Figure 5 is a $\Delta v = 4$ pathway. It corresponds to a near resonant energy transfer that is accompanied by an energy gain to the solvent of less than kT. This process is described as a vibrational energy relaxation process with no accompanying vibrational cooling (VC) in the language of Dlott and co-workers.[4] Inspection of the normal mode frequencies indicates that the nearby candidate states are those that have two quanta in the CH bend and one quantum in the CCl stretch. Although many other states are nearly degenerate, these other states correspond to a larger overall quanta of vibrational energy. For example, states with six quanta of CCl stretch are also nearly degenerate. These have $\Delta v = 7$ and are therefore less likely. There is another possible $\Delta v = 4$ pathway that we have not included in the Figure 5, this being the pathway to states with two quanta of CH bend and one quantum of CCl bend. We note that ΔE is at least three times greater for this process than for the one we have included. An analogous pathway will be more important for the relaxation of the CH overtones, since this pathway will tune into resonance as excitation of the CH increases. The experimental frequency results are consistent with the former of these two $\Delta v = 4$ pathways, since there is little population build up in the Cl−C−Cl bending motions during the first stage of the decay. However, as stated above, the experimental results suggest equal population in the CCl stretches and CH bend fundamentals.

Figure 6 shows similar information for $CHBr_3$. A comparison of the two panels illustrates that the likely acceptor states (shown in the bottom panel) form a small subgroup of the total states (shown in the top panel). This figure contains additional information, since it separates the acceptor states according to the overall change in vibrational quanta. Finally, it also highlights the dense background of nearly degenerate states.

The primary goal of our study is to determine the relative importance of the above pathways and to gain some insights as to the couplings that lead to them. The theoretical tool we employ to this end is semiclassical perturbation theory in which the solute is treated quantum mechanically and the solvent is treated classically. It is clear that the approach detailed in the last few paragraphs is fruitful in interpreting the computed rates, and also detecting any pattern anomalies. With this in mind, we turn our attention to the actual scheme of computations itself.

IV. Theory and Computations

The theoretical framework for the computation of relaxation rates has been elaborated in many articles.[38,39,42−44,79,109] We shall review the scheme, beginning with the treatment of the Hamiltonian for each of the systems considered. Discussions of LT theory and a time-dependent approach follow, which are the two main methods we have employed in the computation of CH and OH stretch relaxation rates.

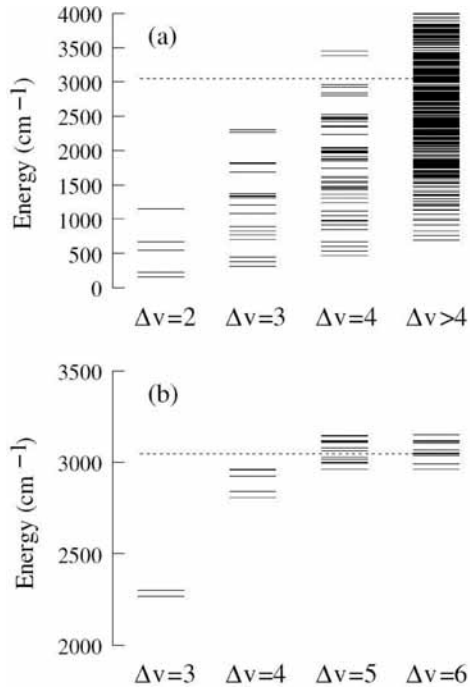

Figure 6. Plot of energies of available acceptor states in $CHBr_3$. Only those states that have no quanta of CH stretch excitation have been shown. The only exception is the CH stretch fundamental (1_1) itself, shown with the long dotted line. (a) States in the 0−4000 cm^{-1} range sorted by the change in number of quanta (Δv) from 1_1. Only states that have 3 quanta or less in the low frequency umbrella and CBr bend modes are shown. (b) Set of candidates chosen for the LT calculation.

A. Partitioning of the Hamiltonian. A formal description of VER between states of a solute molecule in a solvent bath begins with the partitioning of the total Hamiltonian

$$H = H_s + H_b(t) + V(t), \quad V(t) = \langle V \rangle + V'(t) \tag{2}$$

H_s is the solute gas-phase vibrational Hamiltonian containing various anharmonic terms and intramolecular couplings. Our Hamiltonian neglects the small contributions from Coriolis and centrifugal coupling.

The solute eigenstates $\{|i\rangle\}$ are calculated using Van Vleck perturbation theory. We have shown that this approach provides accurate descriptions of low-lying vibrational states for several molecules. The details of this method have been described previously by Wang and Sibert[110] for the CHD_3, Ramesh and Sibert[111] for $CHBr_3$, and Sibert and Castillo-Chará[112] for methanol. These studies require as input an ab initio anharmonic gas phase potential energy surface. One is referred to those works for further details of the calculations.

The bath Hamiltonian, $H_b(t)$, includes the rotations and translations of all molecules (and may also include vibrations of the solvent). The coupling terms in $V(t)$ come from the chosen intermolecular potential. The potentials typically include Lennard-Jones plus Coulomb interactions. We have, at times, included polarization,[43] and in some instances it was necessary to carry out ab initio calculations in order to determine the appropriate intermolecular potential.[50] It should be noted that the challenge of calculating solvent−solute couplings is an outstanding one, and, as such, it is the subject of significant research activity.[57,107,113−118]

As usual, $H_b(t)$ is treated classically and is obtained via molecular dynamics simulations. The bath average of the coupling is given as $\langle V \rangle$. For strongly interacting systems, such as water and methanol, it is crucial to take into account the average influence of the solvent, which involves the use of $H_s + \langle V \rangle$ as the solute Hamiltonian.[42,44] The purpose of this inclusion is to recover the red shift of the positions of the eigenstates, which are seen in condensed phase spectra. For relatively weakly interacting systems, such as chloroform and bromoform, the diagonal matrix element $\langle V_{ii} \rangle$ may be used for a rough estimate of the shift for the state $|i\rangle$. Ramesh and Sibert[50] obtained blue shifts for the states of $CHBr_3$ instead. However, these shifts are no larger than about 10−15 cm^{-1}. The only exception is the CH stretch state, which shows about 5 cm^{-1} of red shift, but still falls well short of the 30 cm^{-1} experimental shift. The blue shifting, which was found in the case of chloroform[43] as well, is usually attributed to the strong short-range repulsive influence and the absence of polarization in the modeled intermolecular potentials.[119] On account of this, we do not include $\langle V \rangle$ in the solute Hamiltonian for the haloforms.

The fluctuating coupling, $V'(t)$, is written out as a Taylor series expansion in terms of normal coordinates (Q)[111]

$$V'(t) = -\sum_i F_i(t) Q_i - \sum_{i<j} F_{ij} Q_i Q_j - \ldots \tag{3}$$

Select third and fourth order terms are also present. At a minimum, we include those terms that would directly couple likely candidate states. Most relaxation studies have employed rectilinear normal coordinates. For computation of isolated molecule energies, the curvilinear set has the advantage of compactness of potential expansions and quicker eigenstate convergence. However, it is not immediately clear which is better suited for VER treatments. Ramesh and Sibert[50] have discussed this issue.

For methanol, the separation between solute and solvent is modified so that the torsional motion is included in the bath. We expect that the motion of the torsion is more strongly coupled to the surrounding molecules than it is to the vibrations of the same molecule. Moreover, in LT theory, the bath degrees of freedom are treated classically, and since the torsion frequency is low, a classical treatment is reasonable.

B. Landau−Teller Theory. The LT method is the standard approach for the computation of rates of vibrational decay.[80] Based on first order perturbation theory, the method involves the calculation of the Fourier transforms (FTs) of time correlation functions of $V'_{ij}(t) = \langle i|V'(t)|j\rangle$. The rate of energy transfer from state $|i\rangle$ to $|j\rangle$ is given as

$$k_{ij} = \frac{B(\omega_{ij}, T)}{\hbar^2} \int_{-\infty}^{\infty} \mathrm{d}t\, \mathrm{e}^{i\omega_{ij}t} \langle V'_{ij}(t) V'_{ji}(0) \rangle \tag{4}$$

Here $\omega_{ij} = (E_i - E_j)/\hbar$, where the $\{E_i\}$ are eigenvalues of H_s. The quantum correction factor (QCF), $B(\omega_{ij}, T)$, is expected to be close to unity in polyatomic systems where near-resonant transfer is possible, i.e., $\omega_{ij} < kT$ for the states of interest. The total rate of decay of population for state $|i\rangle$ is, of course, the sum of the contributing rates k_{ij}.

The LT equations assume that the energy levels are not fluctuating under the influence with the solvent bath. In order in include these fluctuations we implement the fluctuating Landau−Teller (FLT) method, employed by Staib and co-workers[120,121] and more recently by Bakker[122] and Gulmen and Sibert.[45,46] This method is particularly useful when several acceptor states are in close proximity to the relaxing vibration. The FLT rate is computed using the expression

$$k_{ij} = \frac{1}{\hbar^2} \int_{-\infty}^{\infty} \mathrm{d}t\, \mathrm{e}^{i\omega_{ij}t} \langle \cos(\theta_{ij}(t)) V'_{ij}(t) V'_{ji}(0) \rangle \tag{5}$$

The quantity $\theta_{ij}(t) = 1/\hbar \int_0^t \mathrm{d}\tau [V'_{ii}(\tau) - V'_{jj}(\tau)]$ represents the

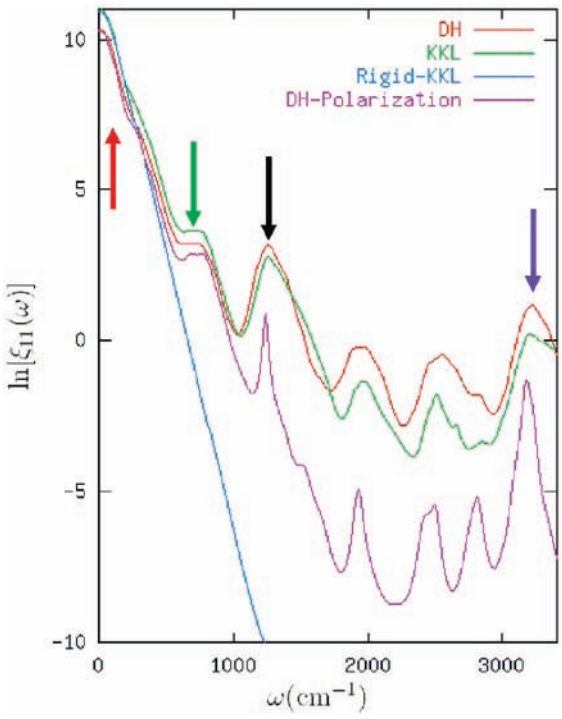

Figure 7. Logarithm of the frictions $\xi_{11}(\omega)$ along CH stretch normal coordinate of chloroform for different intermolecular force fields as a function of ω.

main change in the computation scheme from traditional LT theory. It introduces the effect of solvent-induced level fluctuations into the rate calculations. Further details on this scheme may be found in refs 45 and 46. Since FLT is relatively new and less well-tested, we always compare its results with the LT and/or TD approach.

The friction is an important quantity in LT calculations. It is written as a function of frequency as

$$\xi_{ij}(\omega) = \int_{-\infty}^{\infty} \mathrm{d}t\, \mathrm{e}^{i\omega t} C_{ij}(t),$$
$$C_{ij}(t) = \langle \cos(\theta_{ij}(t)) V_{ij}'(t) V_{ij}'(0) \rangle \qquad (6)$$

Clearly, $\xi_{ij}(\omega = \omega_{ij}) = \hbar^2 k_{ij}$, and $\theta_{ij} = 0$ for standard LT theory. This friction tells us a great deal about the solvent dynamics and the magnitudes of the solute−solvent interactions. Figure 7 shows an example of the (standard LT) friction calculated for a neat solution of chloroform where the all terms in $V'(t)$ have been set to zero except the term linear in the CH stretch normal mode. The curves correspond to different simulation models used. All models shown, save for rigid-KKL, permit the solvent molecules to vibrate with an average energy of kT.[43] It is apparent that the flexible models show peaks at frequencies of the fundamental vibrations and their overtones, whereas the rigid-KKL results rapidly decay to zero as frequency increases.

The four arrows correspond to the energies at which the friction is evaluated to get the rate for each of the four transitions (same color coding) shown in Figure 5. One finds very different rates for the transition from the CH fundamental to the ground state (purple arrow) for the rigid versus flexible KKL force field. Such large differences are usually taken to signal a solute−solvent vibration-vibration (V−V) energy transfer route. At low energies, however, the rigidity is less important, though there are still differences of about a factor of 2 depending on the details of the models [cf. Figure 8]. As we shall see in Sec. 5, the low frequency transition at the red arrow's position is the dominant one.

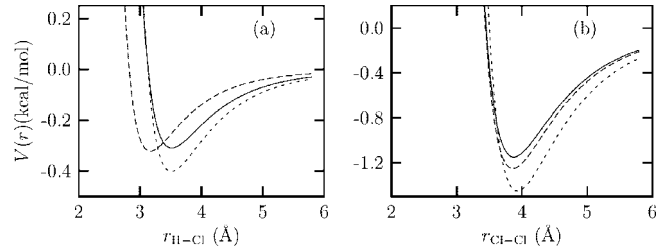

Figure 8. Plot of intermolecular potentials for chloroform versus (a) r_{H-Cl} distance and (b) r_{Cl-Cl} distance for two different force fields used in the simulation, those of Dietz et al.[138] (DH) and Kovacs et al.[139] (KKL). For comparison a third force field, that of Chang et al.[140] (CDP), is also shown. The most notable difference between these force fields is for H−Cl interaction; the DH potential (− −) has an inner wall at a smaller r_{H-Cl} distance than do either the CDP (- -) or KKL (—) potentials. The CDP potential has a more attractive Cl−Cl interaction than the other two.

As noted above, the LT equations assume that the energy levels are not fluctuating under the influence with the solvent bath. Though $\langle V_{ii}' \rangle = 0$ by definition, $V_{ii}'(t) \neq 0$ and coupled states may move closer or further away from each other, hence the energy transfer rates are dynamically enhanced or reduced. This effect is automatically accounted for in a more direct time-dependent approach, which we describe next.

C. Time-Dependent Method. The effect of the solvent-induced fluctuations is adequately captured by FLT, as we shall shortly see. Computationally, it is also not much more demanding than standard LT. A way to independently verify the results of FLT is the time-dependent (TD) method. This method involves the propagation of the coefficients of the eigenstates, c_i, in the Schrödinger equation in matrix form

$$i\hbar\dot{\mathbf{c}} = [\mathbf{H}_s + \mathbf{V}'(t)]\mathbf{c} \qquad (7)$$

The natural presence of the level fluctuations in this equation affords a formal improvement upon the LT approach. Plots of $P_i(t) = \langle |c_i(t)|^2 \rangle$ can be used to extract rates of population decay out of state $|i\rangle$, where $\langle ... \rangle$ indicates averaging over many trajectories.

The TD method is typically carried out for a small set of eigenstates that are expected to be most consequential in the relaxation process. The initialization of the calculation is made as $c_j = \delta_{ij}$, where $|i\rangle$ is the excited state. An alternate method of starting the calculation is to add to V' a laser interaction of the form $-\mu_o Q_1 E(t)$, where

$$E(t) = E_0 \exp[-(t - t_0)^2/T_0^2] \cos(\omega_L t) \qquad (8)$$

The shape and duration of the pulse are controlled by the parameters E_0, t_0, T_0, and center frequency ω_L.[43,44]

In addition to the advantage of a more accurate treatment of the solute, this approach has one positive and one negative feature. The positive feature is that this calculation leads to significant insights into the nature of the relaxation beyond that of LT. Goodyear and Stratt[40] point out that it is important to distinguish between processes that occur for essentially all solute molecules regardless of their surroundings, and processes that may be limited to only a small fraction of the solute molecules but are nonetheless so efficient that they control the relaxation. The time-dependent approach enables us to do this, since solving eq 7 in a basis consisting of the eigenstates of $\hat{H}_s$ allows us to calculate the probability of a CH or OH stretch fundamental being populated as a function of time, and to determine the nature of the collisions that lead to this transfer of probability. The negative feature is that detailed balance is not obeyed. Thus,

when the energy gap is larger than kT, one needs to be concerned about the accuracy of the method.

V. Results and Discussion

Using the tools discussed in the previous sections, we present a summary of the main findings on methanol and haloform relaxation. We avoid many of the details presented in the original articles,[43−46,50−52] and highlight the salient features in each case and trends across these systems. We first present the LT and TD results on haloforms. We then continue on to neat methanol findings with LT and TD theories. Finally, we discuss the computed effects of deuteration and solvent change in methanol. For notational consistency within this review, $\alpha_m\beta_n$ represent a state whose leading character (more precisely, basis function) has m and n quanta of excitation in mode numbers α and β, respectively. Superscripts or additional tags label the symmetry. This notation is not consistently used in the original articles; we hope the reader will not find the translation cumbersome.

A. Haloforms. The study of CH stretch relaxation in neat $CHCl_3$ was the first of our studies.[43] Figure 5 shows the several candidates states to which the energy may flow. It was found that there is a *single* acceptor state, one with 2 quanta in the CH bend and 1 quantum in the symmetric CCl stretch, or $2_14_2(A_1)$. The fact that this states appears as the only acceptor state stood out as one of the most surprising results of the paper by Sibert and Rey.[43] The lifetime for this $\Delta v = 4$ channel was found to be about 12−23 ps, depending on the force field used. These are in excellent agrement with the 23 ps experimental lifetime of the CH stretch due to Graener et al.[10] Furthermore, the results were found to be the same whether the solvent was set to be flexible or rigid. This indicates that the CH relaxation is not accompanied by concomitant vibrational excitation of a neighboring solvent molecule.

The presence of a single acceptor highlights the dominant influence of the rapid decrease in friction with increasing frequency [cf. Figure 7]. The $2_14_2(A_1)$ state lies just 54.5 cm^{-1} above the CH stretch: the energy transfer is near resonant (red arrow in Figure 7). Apparently, the friction falloff is sufficiently fast that the lower Δv pathways are unimportant. The friction plots also explain why the rigid and flexible solvent molecules provide such similar results; the rigid and flexible curves are nearly identical at low frequencies.

Only when one looks at the relative contributions of the minor pathways are large differences found between rigid and flexible solvent models. For example, the rate of flow to the $2_14_1^1$ state, decreases by over 3 orders of magnitude when solvent vibrations are frozen. This minor pathway, marked with the black arrow in Figures 5 and 7, involves relaxation with concomitant vibrational excitation of a solvent. We mention this particular pathway, since the experimental results of Graener et al.[10] suggest that it is the dominant route through which the CH stretch relaxes. Our results, even for the flexible model, clearly indicate that this is unlikely.

Table 2 shows that other fundamentals decay on a wide range of times from 5.4 ps for a Cl−C−Cl bend to 221 ps for the CCl stretch. The C−Cl stretches transfer energy between each other rapidly. However, they lose energy to the solvent on a time scale of 200 ps. The lowest frequency bend has the fastest relaxation rate. The table also shows that, in contrast to the CH stretch decay, the solvent vibrations are at times very important. The difference in rates between the flexible and rigid models is a measure of the importance of a process that includes simultaneous excitation of a solvent vibration. Note, if the rigid and flexible results are similar, only one result is given.

TABLE 2: Select Chloroform LT Rates[43] out of Fundamentals Obtained with KKL Model[a]

fundamental	v	v'	$[k_{ij}]^{-1}$ (ps)	model
CH bend	4_1	3_15_1	71	rigid
	4_1	3_15_1	66	flexible
CCl stretches	2_1	5_1	15	rigid
	2_1	5_1	15	flexible
	2_1	3_1	496	rigid
	2_1	3_1	221	flexible
	5_1	3_1	18000	rigid
	5_1	3_1	2700	flexible
Cl−C−Cl bends	3_1	6_1	25	rigid
	3_1	g.s.	40	rigid
	6_1	g.s.	5.4	rigid

[a] First or second fastest decay routes are shown for each fundamental.

TABLE 3: Landau-Teller Timescales (without QCF) for CH Stretch Population Decay in $CHBr_3$ to Various States[a]

state	ω_{1j} (cm^{-1})	$k_{1,j}^{-1}$ (ps)
$4_15_3(A_1)$	62.4	1018.5
$3_25_16_1(A_1)$	33.8	596.7
$2_24_15_16_1(A_1)$	−1.6	1.6
$2_13_14_2(A_1)$	−17.9	365.3
$2_14_15_2(A_1)$	−30.7	231.2
$2_14_26_1(A_1)$	−51.7	902.9
$2_14_26_1(E)$	−84.3	659.6
$3_32_4(E)$	−85.0	524.4
$4_25_1(A_1)$	−85.7	50.8

[a] The data is from ref 50. Only those states are listed for which the rate $k_{1,j}^{-1}$ is less than 1500 ps. Transition energies ω_{1j} are relative to the CH stretch state, 1_1.

Turning to $CHBr_3$, we calculated that the CH stretch relaxes with a 50 ps experimental time scale, twice as slowly as in $CHCl_3$. The potential acceptor states (Figure 6a) are more numerous than for chloroform owing to the lower frequencies of the Br containing modes. Using the guidelines in section III, these can be whittled down to the more manageable set seen in Figure 6b. In spite of this, the dominant energy flow channel from the CH stretch is again to a single state, namely $4_25_1(A_1)$, a $\Delta v = 4$ acceptor which contains 2 quanta of CH bend and one quantum of asymmetric CBr stretch. The LT rate to this state is 51 or 89 ps, depending on the whether the friction is evaluated at theoretical or experimental transition gap. This pair of rates can be considered as depicting an uncertainty magnitude. Nonetheless, both are in good agreement with the experimental value.

Table 3 shows the stark difference in LT timescales between this mode and other candidates, all of which are $\Delta v > 4$ states. Remarkably, the near-resonant state, labeled $2_24_15_16_1(A_1)$, shows a time scale of 1.6 ps. It turns out that this result is a shortcoming of LT theory, arising from the immobility of the energy levels, and is well worth investigating (as we have[50]). We shall briefly return to it when discussing a similar feature in the results for methanol. Moving past this outlier, we find that $2_14_2(A_1)$, which is a close-lying $\Delta v = 4$ state, is missing from the table: it has too slow an LT rate to be listed. Recall that this is the state that accepted energy in the case of chloroform. The reason for its absence can be understood through Figure 9 that shows the position of $4_25_1(A_1)$ and $2_14_2(A_1)$ in both $CHCl_3$ and $CHBr_3$. The former is always higher in energy than the latter. However, it is the closer of the two to the CH stretch that acts as the main acceptor: The $\gtrsim$100 cm^{-1} difference in the transition gap is sufficient to reduce the friction by a few orders of magnitude and strike out one of them.

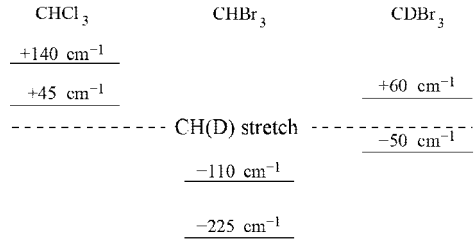

Figure 9. Positions of $4_2 5_1(A_1)$ and $2_1 4_2(A_1)$ in haloforms relative to the CH(D) stretch eigenstate. The former combination state is of higher energy in all molecules. We note that the energy spacings are only estimates based on the experimental fundamentals.[11]

Given that both chloroform and bromoform relaxation are dominated by flow to a single state, one might wonder whether simple solute Hamiltonians exist for describing the intramolecular mixing that must take place for relaxation. Note, if the solute Hamiltonian has no anharmonicity, the relaxation rates are many orders of magnitude slower. Ramesh and Sibert[50] considered such representations for bromoform, and found that, with careful implementation of perturbation theory that incorporates all the off-resonance couplings, the solute Hamiltonian matrix could be drastically reduced to a 3×3 or 4×4 form. Likewise, for chloroform, simple intramolecular couplings responsible for solvent assisted relaxation were identified by Sibert and Rey.[43]

The above results for bromoform and chloroform might have one think that it is straightforward to guess the results for deuterated bromoform based on Figure 9. Seifert et al.[12] have measured that the CD stretch relaxes with a time constant of 25 ps, a value twice faster than that of the CH stretch of bromoform. The two main candidates straddle the CD stretch, which can be loosely thought of as the reason for the rate doubling. It is not so, however, since the intramolecular couplings are substantially more complicated in $CDBr_3$. The CD bend, and hence its overtone, are strongly mixed with CBr stretches and bends.[111,123] No comparable coupling is found for the CH bend. Hence, a plenitude of acceptors replace the two states for $CDBr_3$ shown in Figure 9. The proximity of several candidates made it necessary to explicitly consider level fluctuations using FLT and TD.[51] The rates so computed show that deuteration results in a fundamental change of the relaxation mechanism. The CD stretch moves energy to many states via the solvent coupling, with no single one being dominant. The combined decay time scale using either FLT or TD was found to be about 31 ps,[51] which agrees well with the experimental value of 25 ps measured by Seifert et al.[12] Interestingly, most of the acceptors have $\Delta v \geq 5$.

We redirect the remaining discussion of the haloforms to the TD results. As pointed to in section IV.C, these calculations provide single molecule information. Only after averaging over many solute molecules does one regain the ensemble average results such as that provided by LT theory. A good example of this is shown in Figure 10, where probability flow of the CH stretch of individual chloroform molecules is plotted as a function of time.[43] The results are those of a reduced dimensional solute Hamiltonian that does not include low frequency bending modes. The differing decay curves reflect the different environments of the solute molecules. The correlation between large peaks in the force (right side panels) and the decay in probability (left side panels) indicate that that the strong repulsive Lennard-Jones collisions play a significant role. From an examination of a several trajectories, it appears that these H–Cl collisions are typically collisions with a single Cl atom

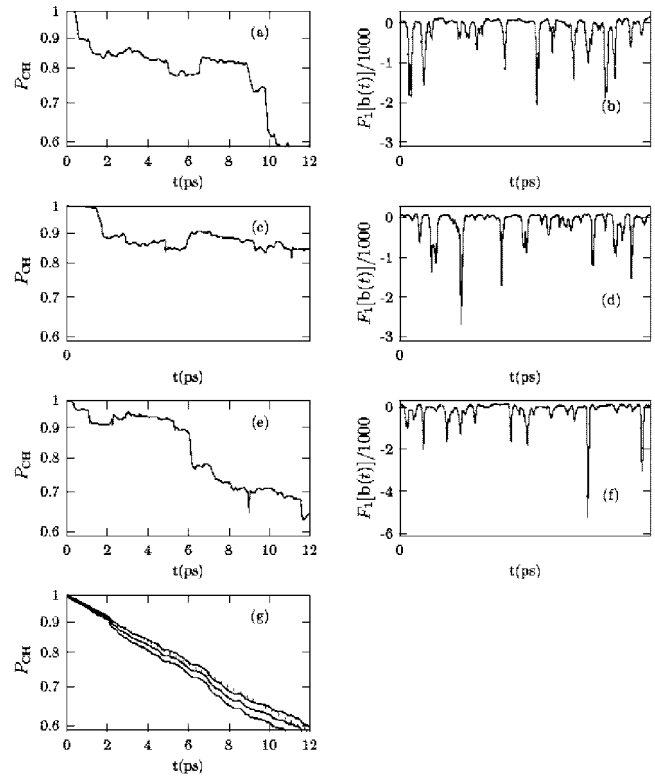

Figure 10. Time-dependent perturbative results for chloroform for P_{CH} as a function of time and F_1 [cf. eq 3] as a function for time for the DH potential. Plots (a), (c), and (e) are for single trajectories. The corresponding force (in units of amu Å/ps^2) along the CH stretch normal mode, F_1 is given in (b), (d), and (f) respectively. The time-dependent ensemble average of P_{CH} is given in (g) along with $P_{CH} \pm \sigma/\sqrt{N}$, where N is the number of trajectories included in the ensemble averaging. The dotted line correspond to exponential decay with lifetimes of $\tau =$ 22.8 ps, which is the corresponding LT lifetime for $B(T) = 1$ for this six dimensional model.

on a neighboring molecule, this being consistent with the H−Cl radial distribution functions. Figure 10g shows that the ensemble averaged result is in excellent agreement with the LT result.

If the TD results always agreed with LT results, the main advantage of TD calculations would be the insights provided by looking at individual trajectories. We have found, however, instances where the two theories give substantially different results. The TD lifetime to the $2_2 4_1 5_1 6_1(A_1)$ state of $CHBr_3$ is 740 ps, compared to the LT result of 1.6 ps reported in Table 3. This is just one example showing that the dynamical fluctuation of the solute energy levels can quench the flow of probability to nearly degenerate states. This phenomenon was discovered using TD calculations to compare results with and without the solvent-induced fluctuations.

B. Vibrational Relaxation of Neat CH_3OH and Dilute $CH_3OH(D)$ in CCl_4. Vibrational relaxation rates in neat methanol are expected to be much faster than that of the haloforms due to stronger intermolecular forces in the H-bonding liquid. Indeed, the experimental results of Figure 2 show that, following OH excitation, many states are populated in a few picoseconds. Surprisingly, upon examination of related systems, one finds that solvent strength is not the only factor: the OD stretch decay rate for CH_3OD in the weakly interacting solvent CCl_4 outstrips, by a factor of at least 10, all the haloform rates discussed above.[55] Apparently, one needs to look more closely at the level spacings and the coupling orders. Following the same approach as was presented for the haloforms, the acceptor states for neat methanol are categorized and plotted as a function

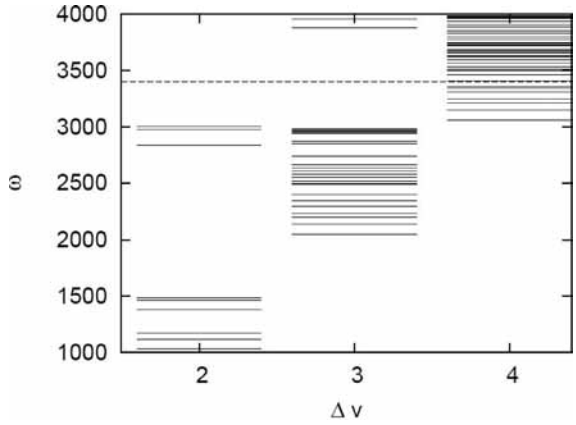

Figure 11. Schematic of vibrational energy levels for MeOH organized by Δv, the total difference in vibrational quanta between a given state and the OH fundamental. The latter's energy is marked with the dashed line.

TABLE 4: Comparison of Liquid Phase Theoretical and Experimental Fundamental Energies[a] for Methanol[44]

state	motion	unadjusted	adjusted	expt.[b]
1_1	OH stretch	3585.4	3400.1	3400
2_1	symmetric CH stretch	2833.1	2833.8	2834
3_1	symmetric CH bend	1468.4	1468.3	1466
4_1	OH bend	1379.8	1381.7	1381
5_1	CO stretch	1052.9	1033.9	1034
6_1	asymmetric CH stretch	3004.5	3004.5	2944
7_1	asymmetric CH bend	1487.1	1487.0	1541
8_1	asymmetric CH_3 rock	1115.6	1115.9	1117
9_1	asymmetric CH stretch	2975.5	2975.4	2944
10_1	asymmetric CH bend	1486.6	1486.6	1541
11_1	asymmetric CH_3 rock	1172.5	1172.4	1117

[a] Theoretical energies (in cm^{-1}) are calculated with second order perturbation theory, both columns including bath averaged solute−solvent potential terms. For better agreement with experimental red-shifts, the OH and CO stretch harmonic frequencies were adjusted and the energies recalculated; see also section IV.A. The experimental frequencies for modes 6−8 cannot be resolved from those of 9−11 and hence are not distinguished in our results. [b] From ref 6.

of energy and Δv in Figure 11. The identities of the states can be gleaned from Figure 1 and Table 4, where the vibrational modes and their frequencies are shown.

The $\Delta v = 2$ processes correspond to transitions to the other 10 fundamentals. Note that the torsion is treated as a classical degree of freedom. If the intermolecular couplings to these modes were the same, then one would expect the CH stretches to be the most important states, since these are the most proximate to the OH stretch. However, in a ball and spring picture, the OH and CH are indirectly coupled through the CO bond, and so one would anticipate small couplings.

Figure 11 shows that there are no near-resonant states with $\Delta v = 3$. In fact, the $\Delta v = 2$ CH fundamentals are closer to the OH stretch. There is a window, almost 1000 cm^{-1} wide, centered around the 3400 cm^{-1} OH stretch fundamental for $\Delta v = 3$. Lying just below this window are the overtones and combinations of CH and OH bends, which have the smallest energy mismatch. Of these states, we anticipate that overtone in the OH bend is likely to be most important, based on the HOD results of Rey and Hynes[38] and Lawrence and Skinner.[42] The states above the window include combination bands with one quantum of CH stretch and one quantum of a methyl rocking mode or CO stretch. Transitions to these states are unlikely, as they require the bath to supply about $2kT$ of energy.

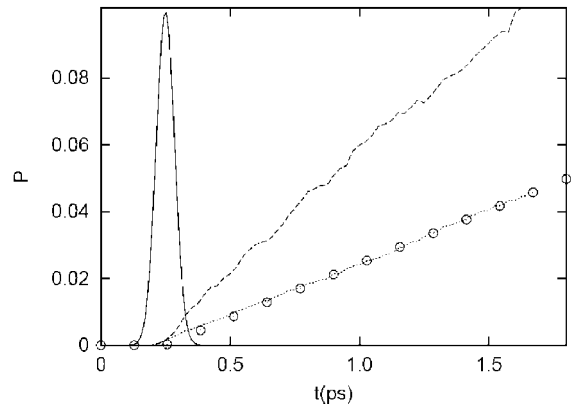

Figure 12. Neat MeOH relaxation results for a 3 state time-dependent calculation that includes the ground state, the 1_1 state, and the 4_2 state. The time dependent laser field, given by eq 8 has $t_0 = 0.25$ ps, $T = 0.05$ ps, and $\omega_L = 3400$ cm^{-1}. The temporal width corresponds to $\Delta\omega = 360$ cm^{-1}. The near impulsive pulse, which is significantly narrower (in time) than that used by Iwaki and Dlott, allows easier comparison to LT results. The dashed curve is the rate of probability flow from the OH fundamental to the COH overtone. The dotted curve is the rate of probability flow between the same states but the diagonal couplings have been reduced by a factor of 15. The points correspond to the LT lifetime result of 29.8 ps.

In contrast to $\Delta v = 3$, there is no gap in the $\Delta v = 4$ states at energies near 3400 cm^{-1}. As one progresses up this stack, one proceeds from states that have three quanta of excitation in the CO stretch and the rocking modes to ones that have two quanta in these modes plus one quantum of excitation in an OH or CH bend. At the higher energies, there are states with one quantum in either the CO stretch or the methyl rock with two quanta in the bending modes. The transition from the OH stretch to any of these, and also that between them, requires only a small amount of energy transfer to or from the bath. Thus, we anticipate that these states may have an important role in the relaxation pathway.

Gulmen and Sibert[44] found that many of the above states were important contributors, yielding an overall OH lifetime of around 2 ps. The lifetime is slower that the experimental one, which is reported as less than 1 ps.[6] A similar slower-than-experiment lifetime was found in theoretical OH decay calculations for HOD in D_2O[38,42] and is presumably a result of the inadequacies of the fixed-charge solute−solvent model employed in those works and ours to describe hydrogen bonding.

A noteworthy effect found in the OH relaxation is that of the solvent assisting the vibrational relaxation via a dynamic shifting of the solute energy levels. A 3-state model that includes the ground state, the fundamental 1_1, and the 4_2 OH bend overtone nicely illustrates this effect. Figure 12 shows that the ensemble averaged TD results are about a factor of 3 faster than the corresponding LT results without the QCF. This effect stems from the diagonal solute−solvent coupling terms, which induce the solute level fluctuations. They are naturally present in a TD calculation but are absent in the standard LT theory. For a verification of these statements, Gulmen and Sibert[44] recalculated the time-dependent rates, reducing the diagonal couplings by a factor of 15. The resulting rates,[44] also shown in Figure 12, are in excellent agreement with LT theory. This comparison points to a serious drawback of LT theory.

When all of the decay channels are included, the overall relaxation rate was essentially the same for the LT and TD results, despite the effect described above. The similarity of these results is due to cancelation of errors. Energy fluctuations can both enhance or diminish relaxation rates. A severe overestima-

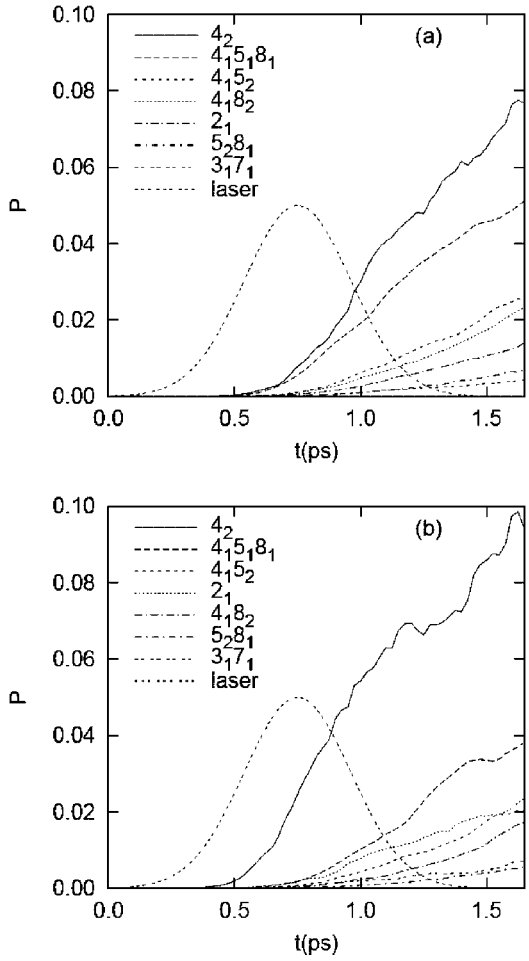

Figure 13. Results for the 9 state TD model for neat MeOH. Laser frequencies in (a) and (b) are centered at $\omega_L = 3400$ and 3250 cm $^{-1}$, respectively. The temporal width, given by $T_o = 0.3$ ps in eq 8 yields a spectral fwhm of 50 cm $^{-1}$. The probability flow into the OH bend overtone is significantly enhanced compared to the other states upon this lowering of the excitation frequency.

tion occurs whenever two solute states are intramolecularly weakly coupled yet mix solely due to near-degeneracy. The mixing drops rapidly as solvent shifts increase the separation between the states. This dynamic decoupling effect was seen by Gulmen and Sibert[44] for a $\Delta v = 4$ state (more below), for which LT theory predicted an anomalously high rate of about 0.05 ps. The effect was seen for $CHBr_3$ as well (see Table 3 and section IV.A). Our LT results exclude this state's contribution when we compare to TD rates.

These fluctuations can also be used to direct energy flow. By using a laser pulse, OH stretches in more strongly or weakly hydrogen bonded environments may be preferentially excited via the choice of ω_L. Following the experiments of Iwaki and Dlott,[6] Gulmen and Sibert[44] used ω_L values of 3250 and 3400 cm^{-1}, where the former excites those molecules for which the hydrogen bond is more likely to be stronger than those with the bluer excitation frequency. The results shown in Figure 13 clearly demonstrate this effect, which is even more pronounced in the experimental work of Iwaki and Dlott.[6]

For all of the advantages of the TD method we just discussed, it is cumbersome to implement compared to the LT approach. Fortunately, the extended LT theory of Bakker[122] offers a solution, wherein energy level fluctuations are included in the zero order Hamiltonian. Applying this FLT theory to methanol OH relaxation, good agreement with TD results was observed

TABLE 5: Time Constants (ps) out of the ν (OH) State for Neat MeOH Calculated with TD, LT, and FLT Theories[a]

state	ω	TD	LT	FLT
5_28_1	249.4	9.4	30.3	15.1
4_2	665.3	13.9	29.8	11.8
$4_15_18_1$	−98.0	14.9	20.1	15.1
4_18_2	−191.6	38.0	160	46.3
4_15_2	−5.6	65.9	0.05	51.8
9_1	566.3	156	616	441
3_17_1	415.4	425	807	517
total		3.4	8.0[b]	3.8

[a] The average energy ω separating 1_1 from presented state is in wavenumbers. [b] Without contribution of state 4_15_2.

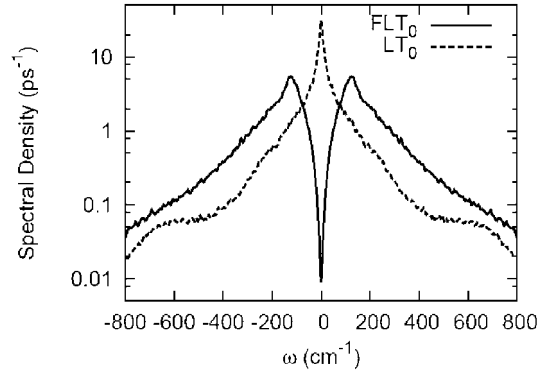

Figure 14. Spectral density for the 4_15_2 state in neat MeOH calculated through the use of LT theory and the FLT theory are presented in units of the rate constant (ps^{-1}) versus frequency difference (cm^{-1}). The 0 subscript indicates that no quantum correction factor was used.

for many states.[45] Comparisons of FLT theory with TD and LT results are shown in Table 5 for seven methanol acceptor states. No quantum correction factors are included. The most notable differences are in the LT and TD or FLT rates for the nearly degenerate state 4_15_2, which are 0.05 and 66 ps, respectively. The slower TD and FLT timescales are a result of the dynamical decoupling described above. The FLT result of eq 6 dramatically modifies the friction for this state, as shown in Figure 14, especially at low frequencies, thereby removing the LT overestimation artifact.

To explore the role of solvent environment, relaxation of the OH(D) stretch fundamentals of monomeric MeOH and MeOD in CCl_4 solvent have been investigated. Sibert and Gulmen[46] calculated lifetimes of 4−8 and 2−3 ps, respectively. These results agree well with the respective experimental values of 9[56] and 2 ps.[55] The energy level patterns of the solute molecule in the average force field of the solvent, shown in Figure 15, help elucidate these results. The relevant acceptor states are found to lie in the windows marked by the boxes. The positions of these boxes show that both systems display energy transfer to modes that are nearly degenerate to the OH(D) stretch state marked with a bold red line. However, the OD stretch is nearly resonant with $\Delta v = 3$ states while the OH stretch is nearly resonant with $\Delta v = 4$ states. Hence, the former displays stronger couplings, and the acceptor states span a greater energy window. The weaker $\Delta v = 4$ transitions lead to slower MeOH relaxation. Note that the smaller Δv value more than compensates for the decreased coupling expected a result of deuteration. Also shown in Figure 15 are results for relaxation in neat MeOH. There the hydrogen bonding solute−solvent interactions are stronger, and even though there are many $\Delta v = 4$ transitions, $\Delta v = 3$ transitions are significant.

These results are quantified in Figure 16 where state-to-state relaxation rates are plotted versus energy difference between

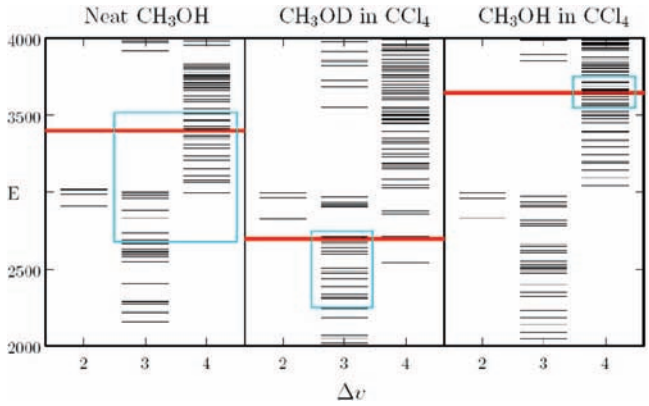

Figure 15. Energy levels of MeOH and MeOD in different solvents, organized as a function of Δv, the difference in vibrational quanta between the initial OH(D) stretch state and the acceptor state. Bold (red) lines indicate OH(D) stretch fundamentals. Significant acceptor states are shown in boxes. Fast energy flow in CH_3OD in CCl_4 is due to near resonant $\Delta v = 3$ states.

initial and final states for methanol. If chloroform and *h*-bromoform results were included, they would consist of plots with a single line since there is one acceptor state in the CH stretch relaxation. For methanol, many states are populated. The most surprising result is that neat CH_3OH and dilute CH_3OD in CCl_4 look remarkably similar. We understand this result based on the fact there are numerous $\Delta v = 3$ states nearly degenerate for the latter solute but not the former [cf. Figure 15]. This result is consistent with the $\Delta v = 4$ dominated results of CH_3OH in CCl_4 where energy flows into a narrow band of nearly degenerate states. A loose comparison may also be made between CH_3OH in CCl_4 and neat $CDBr_3$ based on the top panel of the figure. The analogous picture for *d*-bromoform would likely appear similar, with acceptors clustered about the relaxing state. The common feature of these two systems is that, while the solute−solvent interactions are weak, the rate is still fairly high because of the availability of several decay channels. This acceptor multiplicity is possibly in both solutes owing to sizable intramolecular couplings.

Finally, we comment on the sensitivity of these results to the positions of the states in Figure 15. As in the bromoform calculation, the CH_3OH in CCl_4 results are sensitive to these positions, and for this reason we report here results between 4 and 8 ps. This range arises from estimates in the uncertainties of certain $\Delta v = 4$ states. The neat methanol and dilute CH_3OD in CCl_4 are less sensitive to the details of the potential. In the former, the large solvent-induced fluctuations reduce the sensitivity of the average line positions. In the latter, the larger couplings and lower density of states associated with $\Delta v = 3$ processes also reduce the sensitivity of the final rates on the solute eigenstates.

Briefly summarizing, this section and the prior ones review our recent contributions to the understanding of condensed phase vibrational energy flow patterns. A central feature of our work is the study of molecules with large numbers of acceptor states, and where near resonant energy flow is prevalent. We have shown that the structure of the energy levels, as shown in Figures 6, 9, 11, and 15 are an essential tool for interpreting flow rates. Solvent-induced fluctuations in the solvent energy levels may critically affect decay rates, so it is important to go beyond LT theory and include these fluctuations using TD or FLT theories. Finally, in order to get reliable predictions, accurate calculations of the solute eigenstates are needed in addition to good descriptions of the solute−solvent couplings.

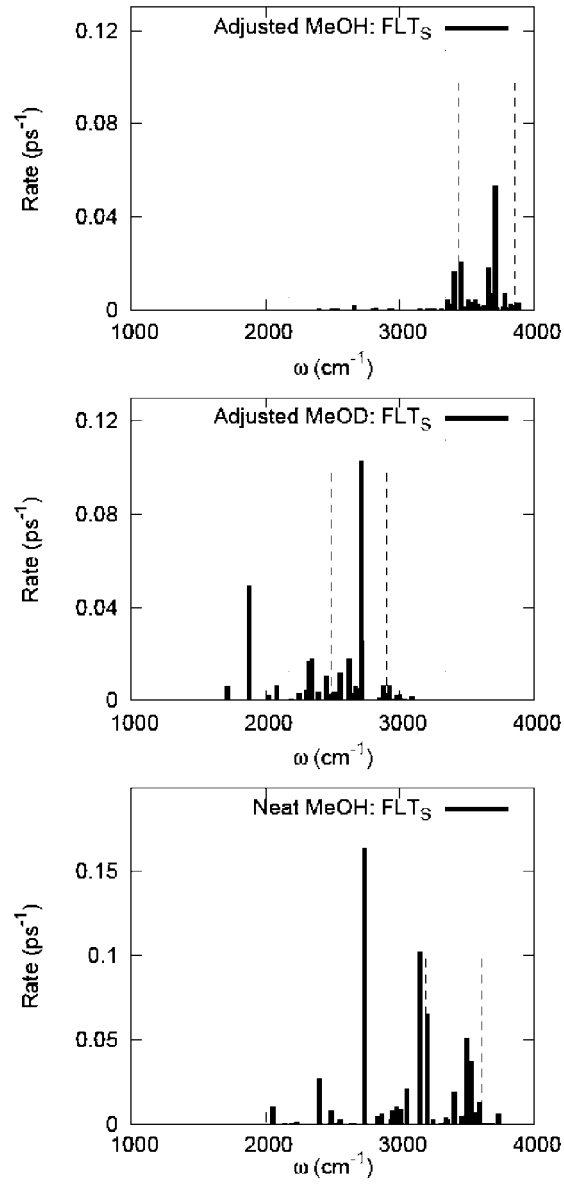

Figure 16. Comparison of the states-to-state relaxation rates (ps^{-1}) versus energy (cm^{-1}) for dilute MeOH and MeOD in CCl_4 and neat MeOH.[44,46] The $\pm k_B T$ band is indicated by the thin dotted vertical lines. Results obtained with the standard quantum correction factor used by Oxtoby.[80]

VI. Future Directions

In the remainder of this paper, we turn our attention more broadly to the issue of future directions. The field of vibrational relaxation is intimately tied to many processes, if not all, involving nuclear dynamics in the condensed phase. A comprehensive discussion of the shape it will assume in the years to come is clearly not possible. We, therefore, limit our comments below to just three areas that we believe to be germane to current progress in the field.

Relaxation studies are steadily shifting away from liquids to interfaces, confined environments, or generally more heterogeneous surroundings. For example, investigators have recently looked at vibrational dynamics of ice in reverse micelles,[5,75,76] nanodroplets,[124] molecular monolayers,[77] and water at interfaces.[27] Much environment-specific information can be garnered from measurements on the probe species, such as its line shape, spectral diffusion and anisotropy, population relaxation, and contrasting them with those in a reference isotropic (bulk)

medium. These would need the use of nonlinear and interface-sensitive detection techniques.[54,70,72−74] A major theoretical challenge in this arena is that, in general, the solvent couplings that underlie population relaxation calculations are obtained from simulations. One must be circumspect about the simulation force fields whenever they are applied to novel environments such as those mentioned above. Usually the force fields need to be refined,[50,57,107,113−118,125,126] and this can be very time-consuming. While there has been considerable success in the calculation of spectral lineshapes, extending such forces fields to population relaxation studies is more demanding since both diagonal and off-diagonal solute−solvent coupling contributions to the solute Hamiltonian need to be computed. Lin et al. proposed a self-consistent procedure for iteratively improving solute−solvent force fields and demonstrated the utility of the method in a study of the relaxation of the bend fundamental of H_2O in chloroform and deuterated chloroform using ab initio dimer calculations to calibrate the accuracy of the fit.

Theoretical treatments of vibrational relaxation typically consider a quantum solute interacting with a classical bath, evolved in time using standard molecular dynamics. For some relaxation processes, particularly for small solutes, pivotal quantum mechanical effects need to be incorporated. The initial value representation provides a useful framework in this regard.[99,127−132] Geva and co-workers and have investigated these quantum effects in a series of papers.[91,98,99,102,132−134] These workers use quantum-mechanical force-force correlation functions obtained from a linearization of the forward−backward action in the semiclassical initial value representation approximation. This approach is equivalent to using a correlation function expressed in terms of the Wigner transforms of both the force and the product of the Boltzmann operator and the force. The resulting multidimensional integrals are costly to evaluate, so further approximations are needed. These integrals are evaluated by the introduction of a local harmonic approximation. While it is difficult to quantify the accuracy of these models, the results offer a promising path for future investigations were quantum effects are significant.

The past few years have seen experimental works that highlight the competition between gas phase-like, solvent independent relaxation and solvent driven relaxation (see also section II, last paragraph). For example, Crim and workers[21,135] find that the rate at which energy leaves the CH stretch of CH_3I is solvent sensitive at the fundamental excitation level, but independent of solvent (and faster) at the first overtone level. Thus far, there has been little theoretical work along these comparative lines. Accurate calculations of vibrational states, needed for a detailed treatment, are stymied due to high state densities around the overtones in solutes that show the above effect. However, not all of the states near the excited one are relevant at the initial decay stage, sometimes even when there is solvent dependence of the decay rate.[20] Returning to Figure 9, one can guess that relaxation following excitation of the CH overtone is significantly faster than that for the fundamental, since the anharmonicity of the OH stretch causes a tuning of the states analogous to those of Figure 9 for the overtone relaxation. Indeed, the lifetime is on the order of a picosecond[51] for the overtone compared to 50 ps for the fundamental. Classical nonequilibrium molecular dynamics yield comparable results.[52] In order to extend our gas phase calculations to the overtone level, we have combined Van Vleck perturbation theory and iterative techniques for obtaining eigenstates[136] to examine the analogous gas-phase relaxation. While the fundamental relaxes much more slowly in than the gas phase[51] than it does in the neat liquid, recent studies in our group on the overtone, show that there is a fast component to gas phase relaxation on the same ps time scale as that observed in the liquid. This work is just one example of the significant influence of intramolecular energy flow in the condensed phase. Of course, bromoform is one of many possible solutes that can be investigated. The systems considered in related experiments over the past decade[17−21,25,32,67,135] clearly exhibit very rich and mixed behavior, and much work remains to be undertaken toward understanding them.

Acknowledgment. This material is based upon work supported by the National Science Foundation under Grant No. CHE 0615165. E.L.S. gratefully acknowledges insightful conversations with Professors Rossend Rey, James Skinner, and James Hynes.

References and Notes

(1) Morresi, A.; Mariani, L.; Distefano, M. R.; Giorgini, M. G. *J. Raman Spectrosc.* **1995**, *26*, 179–216.
(2) Nienhuys, H. K.; Woutersen, S.; van Santen, R. A.; Bakker, H. J. *J. Chem. Phys.* **1999**, *111*, 1494–1500.
(3) Deak, J. C.; Rhea, S. T.; Iwaki, L. K.; Dlott, D. D. *J. Phys. Chem. A* **2000**, *104*, 4866–4875.
(4) Deàk, J. C.; Iwaki, L. K.; Rhea, S. T.; Dlott, D. D. *J. Raman Spectrosc.* **2000**, *31*, 263–274.
(5) Deak, J. C.; Pang, Y. S.; Sechler, T. D.; Wang, Z. H.; Dlottt, D. D. *Science* **2004**, *306*, 473–476.
(6) Iwaki, L. K.; Dlott, D. D. *J. Phys. Chem. A* **2000**, *104*, 9101–9112.
(7) Wang, X.-G.; Sibert, E. L. *Spectrochim. Acta Part A* **2002**, *58*, 863–872.
(8) Bakker, H. J.; Planken, P.; Kuipers, L.; Lagendijk, A. *J. Chem. Phys.* **1991**, *94*, 1730–1739.
(9) van den Broek, M.; Bakker, H. J. *Chem. Phys.* **2000**, *253*, 157–164.
(10) Graener, H.; Zürl, R.; Hofmann, M. *J. Phys. Chem. A* **1997**, *101*, 1745–1749.
(11) Seifert, G.; Zürl, R.; Patzlaff, T.; Graener, H. *J. Chem. Phys.* **2000**, *112*, 6349–6354.
(12) Seifert, G.; Patzlaff, T.; Graener, H. *J. Chin. Chem. Soc.* **2000**, *47*, 667–672.
(13) Graener, H.; Patzlaff, T.; Kadarisman, N.; Seifert, G. *Chem. Phys. Lett.* **2001**, *348*, 403–410.
(14) Seifert, G.; Kadarisman, N. *Chem. Phys.* **2003**, *288*, 113–121.
(15) Graener, H.; Patzlaff, T.; Paradowska-Moszkowska, K.; Seifert, G. *J. Chem. Phys.* **2003**, *119*, 8537–8541.
(16) Seifert, G.; Patzlaff, T.; Graener, H. *J. Chem. Phys.* **2004**, *120*, 8866–8867.
(17) Yoo, H. S.; Dewitt, M. J.; Pate, B. H. *J. Phys. Chem. A* **2004**, *108*, 1348–1364.
(18) Yoo, H. S.; Dewitt, M. J.; Pate, B. H. *J. Phys. Chem. A* **2004**, *108*, 1365–1379.
(19) Yoo, H. S.; Mcwhorter, D. A.; Pate, B. H. *J. Phys. Chem. A* **2004**, *108*, 1380–1387.
(20) Elles, C. G.; Bingemann, D.; Heckscher, M. M.; Crim, F. F. *J. Chem. Phys.* **2003**, *118*, 5587–5595.
(21) Elles, C. G.; Cox, M. J.; Crim, F. F. *J. Chem. Phys.* **2004**, *120*, 6973–6979.
(22) Cox, M. J.; Crim, F. F. *J. Phys. Chem. A* **2005**, *109*, 11673–11678.
(23) Nibbering, E. T. J.; Elsaesser, T. *Chem. Rev.* **2004**, *104*, 1887.
(24) Pakoulev, A.; Wang, Z. H.; Pang, Y. S.; Dlott, D. D. *Chem. Phys. Lett.* **2003**, *380*, 404–410.
(25) Elles, C. G.; Crim, F. F. *Annu. Rev. Phys. Chem.* **2006**, *57*, 273–302.
(26) Seifert, G.; Patzlaff, T.; Graener, H. *J. Chem. Phys.* **2006**, *125*.
(27) Wang, Z. H.; Pang, Y.; Dlott, D. D. *J. Phys. Chem. B* **2006**, *110*, 20115–20117.
(28) Fujisaki, H.; Zhang, Y.; Straub, J. E. *J. Chem. Phys.* **2006**, *124*, 144910.
(29) Pang, Y.; Deak, J. C.; Huang, W. T.; Lagutchev, A.; Pakoulev, A.; Patterson, J. E.; Sechler, T. D.; Wang, Z. H.; Dlott, D. D. *Int. Rev. Phys. Chem.* **2007**, *26*, 223–248.
(30) Seifert, G.; Graener, H. *J. Chem. Phys.* **2007**, *127*.
(31) Shigeto, S.; Dlott, D. D. *Chem. Phys. Lett.* **2007**, *447*, 134–139.
(32) Shipman, S. T.; Douglass, P. C.; Yoo, H. S.; Hinkle, C. E.; Mierzejewski, E. L.; Pate, B. H. *Phys. Chem. Chem. Phys.* **2007**, *9*, 4572–4586.

(33) Smits, M.; Ghosh, A.; Bredenbeck, J.; Yamamoto, S.; Muller, M.; Bonn, M. N. *J. Phys.* **2007**, *9*, 390.
(34) Shigeto, S.; Pang, Y.; Fang, Y.; Dlott, D. D. *J. Phys. Chem. B* **2008**, *112*, 232–241.
(35) Whitnell, R. M.; Wilson, K. R.; Hynes, J. T. *J. Chem. Phys.* **1992**, *96*, 5354–5369.
(36) Kenkre, V. M.; Tokmakoff, A.; Fayer, M. D. *J. Chem. Phys.* **1994**, *101*, 10618–10629.
(37) Moore, P.; Tokmakoff, A.T.; Keyes, D.; Fayer, M. *J. Chem. Phys.* **1995**, *103*, 3325–3334.
(38) Rey, R.; Hynes, J. T. *J. Chem. Phys.* **1996**, *104*, 2356–2368.
(39) Hynes, J. T.; Rey, R. In *Ultrafast Raman and Infrared Spectroscopy*; Fayer., M., Ed.; Marcel Dekker: New York, 2001.
(40) Goodyear, G.; Stratt, R. M. *J. Chem. Phys.* **1997**, *107*, 3098–3120.
(41) Graham, P. B.; Matus, K. J. M.; Stratt, R. M. *J. Chem. Phys.* **2004**, *121*, 5348–5355.
(42) Lawrence, C. P.; Skinner, J. L. *J. Chem. Phys.* **2002**, *117*, 5827.
(43) Sibert, E. L.; Rey, R. *J. Chem. Phys.* **2002**, *116*, 237–257.
(44) Gulmen, T. S.; Sibert, E. L. *J. Phys. Chem. A* **2004**, *108*, 2389–2401.
(45) Gulmen, T. S.; Sibert, E. L. *J. Phys. Chem. A* **2005**, *109*, 5777–5780.
(46) Gulmen, T. S.; Sibert, E. L. *J. Chem. Phys.* **2005**, *123*, 204508.
(47) Leitner, D. M. *J. Phys. Chem. A* **2002**, *106*, 10870.
(48) Fujisaki, H.; Straub, J. E. *Proc. Natl. Acad. Sci.* **2005**, *102*, 6726–6731.
(49) Laage, D.; Demirdjian, H.; Hynes, J. T. *Chem. Phys. Lett.* **2005**, *405*, 453–458.
(50) Ramesh, S. G.; Sibert, E. L. *J. Chem. Phys.* **2006**, *124*, 234501.
(51) Ramesh, S. G.; Sibert, E. L. *J. Chem. Phys.* **2006**, *125*, 244512.
(52) Ramesh, S. G.; Sibert, E. L. *J. Chem. Phys.* **2006**, *125*, 244513.
(53) Wang, Z. H.; Pang, Y. S.; Dlott, D. D. *J. Phys. Chem. A* **2007**, *111*, 3196–3208.
(54) Sovago, M.; Kramer, R. C. H. G. W. W.; Muller, M. J. H. B.; Bonn, M. *Phys. Rev. Lett.* **2008**, *100*, 173901.
(55) Levinge, N. E.; Davis, P. H.; Fayer, M. D. *J. Chem. Phys.* **2001**, *115*, 9352–9360.
(56) Laenen, R.; Simeonidis, K. *Chem. Phys. Lett.* **1999**, *299*, 589–596.
(57) Lin, Y. S.; Ramesh, S. G.; Shorb, J. M.; Sibert, E. L.; Skinner, J. L. *J. Phys. Chem. B* **2008**, *112*, 390–398.
(58) Alfano, R. R.; Shapiro, S. L. *Phys. Rev. Lett.* **1972**, *29*, 1655–1658.
(59) Laubereau, A.; der Linde, D. V.; Kaiser, W. *Phys. Rev. Lett.* **1972**, *28*, 1162–1165.
(60) Spanner, K.; Laubereau, A.; Kaiser, W. *Chem. Phys. Lett.* **1976**, *44*, 88–92.
(61) Laubereau, A.; Fischer, S. F.; Spanner, K.; Kaiser, W. *Chem. Phys.* **1978**, *31*, 335–344.
(62) Myers, D. J.; Chen, S.; Shigeiwa, M.; Cherayil, B. J.; Fayer, M. D. *J. Chem. Phys.* **1998**, *109*, 5971–5979.
(63) Myers, D. J.; Fayer, M. S. M. D.; Cherayil, B. J. *Chem. Phys. Lett.* **1999**, *313*, 592–599.
(64) Dek, J. C.]?>; Iwaki, L. K.; Dlott, D. D. *J. Phys. Chem. A* **1998**, *102*, 819–8201.
(65) Sagnella, D. E.; Straub, J. E. *Biophys. J.* **1999**, *77*, 70–84.
(66) Deàk, J. C.; Iwaki, L. K.; Dlott, D. D. *J. Phys. Chem. A* **1999**, *103*, 971–979.
(67) Bingemann, D.; King, A. M.; Crim, F. F. *J. Chem. Phys.* **2000**, *113*, 5018.
(68) Woutersen, S.; Mu, Y.; Stock, G.; Hamm, P. *Chem. Phys.* **2001**, *266*, 137–147.
(69) Loparo, J. J.; Roberts, S. T.; Tokmakoff, A. *J. Chem. Phys.* **2006**, *125*, 194521.
(70) Mukherjee, P.; Kass, I.; Arkin, I.; Zanni, M. T. *Proc. Natl. Acad. Sci.* **2006**, *103*, 3528–3533.
(71) Deflores, L. P.; Ganim, Z.; Ackley, S. F.; Chung, H. S.; Tokmakoff, A. *J. Phys. Chem. B* **2006**, *110*, 18973–18980.
(72) Botan, V.; Backus, E. H. G.; Pfister, R.; Moretto, A.; Crisma, M.; Toniolo, C.; Nguyen, P. H.; Stock, G.; Hamm, P. *Proc. Natl. Acad. Sci.* **2007**, *104*, 12749–12754.
(73) Park, S.; Moilanen, D. E.; Fayer, M. D. *J. Phys. Chem. B* **2008**, *112*, 5279–5290.
(74) Kwak, K.; Rosenfeld, D. E.; Fayer, M. D. *J. Chem. Phys.* **2008**, *128*, 204505.
(75) Dokter, A. M.; Woutersen, S.; Bakker, H. J. *J. Chem. Phys.* **2007**, *126*, 124507.
(76) Dokter, A. M.; Petersen, C.; Woutersen, S.; Bakker, H. J. *J. Chem. Phys.* **2008**, *128*.
(77) Carter, J. A.; Wang, Z. H.; Dlott, D. D. *J. Phys. Chem. A* **2008**, *112*, 3523–3529.
(78) Miller, D. W.; Adelman, S. A. *Int. Rev. in Phys. Chem.* **1994**, *13*, 359.
(79) Oxtoby, D. W. *Annu. Rev. Phys. Chem.* **1981**, *32*, 77–101.
(80) Oxtoby, D. W. *Annu. Rev. Phys. Chem.* **1981**, *47*, 487–519.
(81) Nesbitt, D. J.; Hynes, J. T. *J. Chem. Phys.* **1982**, *76*, 6002–6014.
(82) Heilweil, E. J.; Doany, F. E.; Moore, R.; Hochstrasser, R. M. *J. Chem. Phys.* **1982**, *76*, 5632–5634.
(83) Chesnoy, J.; Gale, G. M. *Ann. Phys.* **1984**, *9*, 893–949.
(84) Hamm, P.; Lim, M.; Hochstrasser, R. M. *J. Chem. Phys.* **1997**, *107*, 10523–10531.
(85) Gnanakaran, S.; Hochstrasser, R. M. *J. Chem. Phys.* **1996**, *105*, 3486–3496.
(86) Rey, R.; Hynes, J. T. *J. Chem. Phys.* **1998**, *108*, 142.
(87) Egorov, S. A.; Everitt, K. F.; Skinner, J. L. *J. Phys. Chem. A* **1999**, *103*, 9494–9499.
(88) Everitt, K. F.; Skinner, J. L.; Ladanyi, B. M. *J. Chem. Phys.* **2002**, *116*, 179–183.
(89) Shi, Q.; Geva, E. *J. Phys. Chem. A* **2003**, *107*, 9070–9078.
(90) Li, S.; Thompson, W. H. *J. Phys. Chem. A* **2003**, *107*, 8696–8704.
(91) Navrotskaya, I.; Geva, E. *J. Phys. Chem. A* **2007**, *111*, 460–467.
(92) Bader, J. S.; Berne, B. J. *J. Chem. Phys.* **1994**, *100*, 8359.
(93) Egorov, S. A.; Skinner, J. L. *J. Chem. Phys.* **2000**, *112*, 275–281.
(94) Egorov, S. A.; Skinner, J. L. *Chem. Phys. Lett.* **1998**, *293*, 469.
(95) Skinner, J. L.; Park, K. *J. Phys. Chem. B* **2001**, *105*, 6716.
(96) Nikitin, E. E.; Troe, J. *Phys. Chem. Chem. Phys.* **2006**, *8*, 2012–2016.
(97) Poulsen, J. A.; Rossky, P. J. *J. Chem. Phys.* **2001**, *115*, 8024–8031.
(98) Qiang, S.; Geva, E. *J. Chem. Phys.* **2003**, *119*, 9030.
(99) Shi, Q.; Geva, E. *J. Phys. Chem. A* **2003**, *107*, 9059–9069.
(100) Ka, B. J.; Geva, E. *J. Phys. Chem. A* **2006**, *110*, 13131–13138.
(101) Ka, B. J.; Geva, E. *J. Phys. Chem. A* **2006**, *110*, 9555–9567.
(102) Navrotskaya, I.; Geva, E. *J. Chem. Phys.* **2007**, *127*.
(103) Bastida, A.; Cruz, C.; Zuniga, J.; Requena, A.; Miguel, B. *J. Chem. Phys.* **2007**, *126*, 014503.
(104) Morita, A.; Kato, S. *J. Chem. Phys.* **1998**, *109*, 5511–5523.
(105) Lawrence, C. P.; Skinner, J. L. *J. Chem. Phys.* **2003**, *118*, 264.
(106) Li, S. Z.; Schmidt, J. R.; Skinner, J. L. *J. Chem. Phys.* **2006**, *125*.
(107) Li, S. Z.; Schmidt, J. R.; Corcelli, S. A.; Lawrence, C. P.; Skinner, J. L. *J. Chem. Phys.* **2006**, *124*, 204110.
(108) Bakker, H. J.; Planken, P.; Lagendijk, A. *Nature* **1990**, *347*, 745–747.
(109) Velsko, S.; Oxtoby, D. W. *J. Chem. Phys.* **1980**, *72*, 2260–2263.
(110) Wang, X. G.; Sibert, E. L. *J. Chem. Phys.* **1999**, *111*, 4510–4522.
(111) Ramesh, S. G.; Sibert, E. L. *J. Chem. Phys.* **2004**, *120*, 11011–11025.
(112) Sibert, E. L.; Castillo-Chará, J. *J. Chem. Phys.* **2005**, *122*, 194306.
(113) Schmidt, J. R.; Corcelli, S. A.; Skinner, J. L. *J. Chem. Phys.* **2004**, *121*, 8887–8896.
(114) Li, H.; Gordon, M. S. *J. Chem. Phys.* **2007**, *126*, 124112.
(115) Slipchenko, L. V.; Gordon, M. S. *J. Comput. Chem.* **2007**, *28*, 276–291.
(116) Kemp, D. A.; Gordon, M. S. *J. Phys. Chem. A* **2008**, *112*, 4885–4894.
(117) Auer, B. M.; Skinner, J. L. *J. Chem. Phys.* **2008**, *128*, 224511.
(118) Kwac, K.; Lee, K. K.; Han, J. B.; Oh, K. I.; Cho, M. *J. Chem. Phys.* **2008**, *128*, 105106.
(119) Frankland, S. J. V.; Maroncelli, M. *J. Chem. Phys.* **1999**, *110*, 1687.
(120) Staib, A.; Borgis, D. *J. Chem. Phys.* **1995**, *103* (7), 2642–2655.
(121) Staib, A. *J. Chem. Phys.* **1998**, *108* (11), 4554–4562.
(122) Bakker, H. J. *J. Chem. Phys.* **2004**, *121*, 10088.
(123) Fernandez-Liencres, M. P.; Navarro, A.; Lopez, J. J.; Fernandez, M.; Szalay, V.; de los Arcos, T.; Garcia-Ramos, J. V.; Escribano, R. M. *J. Phys. Chem.* **1996**, *100*, 16058–16065.
(124) Dokter, A. M.; Woutersen, S.; Bakker, H. J. *Phys. Rev. Lett.* **2005**, *94*, 178301.
(125) Yang, S.; Cho, M. *J. Chem. Phys.* **2005**, *123*, 134503.
(126) Oh, K. I.; Choi, J. H.; Lee, J. H.; Han, J. B.; Lee, H.; Cho, M. *J. Chem. Phys.* **2008**, *128*, 154504.
(127) Makri, N.; Nakayama, A.; Wright, N. J. *J. Theo. Comp. Chem.* **2004**, *3*, 391–417.
(128) Miller, W. H. *J. Chem. Phys.* **2006**, *125*, 132305.
(129) Bukhman, E.; Makri, N. *J. Phys. Chem. A* **2007**, *111*, 11320–11327.
(130) Liu, J.; Miller, W. H. *J. Chem. Phys.* **2007**, *127*, 114506.
(131) Venkataraman, C.; Miller, W. H. *J. Chem. Phys.* **2007**, *126*, 094104.
(132) Hanna, G.; Geva, E. *J. Phys. Chem. B* **2008**, *112*, 4048–4058.
(133) Ka, B. J.; Shi, Q.; Geva, E. *J. Phys. Chem. A* **2005**, *109*, 5527–5536.
(134) Navrotskaya, I.; Geva, E. *J. Chem. Phys.* **2007**, *127*, 054504.

(135) Heckscher, M. M.; Sheps, L.; Bingemann, D.; Crim, F. F. *J. Chem. Phys.* **2002**, *117*, 8917.

(136) Sprague, M. N.; Ramesh, S. G.; Sibert, E. L. *J. Chem. Phys.* **2006**, *124*, 114307.

(137) Molecular vibrational frequencies Shimanouchi, T. in NIST Chemistry WebBook, NIST Standard Reference Dafase Number 69, Eds. Linstrom P. J. and Mallard, W. G. March 2003. National Institute of Standards and Technology, Gaithersburg, MD, 2003; http://webbook.nist.gov.

(138) Dietz, W.; Heinzinger, K. *Ber. Bunsenges. Phys. Chem.* **1984**, *88*, 968–977.

(139) Kovacs, H.; Kowalewski, J.; Laaksonen, A. *J. Phys. Chem.* **1990**, *94*, 7378–7385.

(140) Chang, T. M.; Dang, L. X.; Peterson, K. A. *J. Phys. Chem. B* **1997**, *101*, 3413–3419.

JP8068442